Integral Error-Based Adaptive Neural Identifier for Nonlinear Lateral Tire Forces

1st Donghwa Hong
Department of Mechanical and Robotics Engineering
Gwangju Institute of Science and Technology (GIST)
Gwangju, Republic of Korea
fairytalef00@gm.gist.ac.kr

2nd Kyunghwan Choi
Cho Chun Shik Graduate School of Mobility
Korea Advanced Institute of Science and Technology (KAIST)
Daejeon, Republic of Korea
kh.choi@kaist.ac.kr

***Abstract*—This paper presents an integral error-based adaptive neural identifier for online estimation of nonlinear lateral tire forces in vehicle dynamics. The adaptive law is derived from an exponentially weighted integral cost functional, which introduces a filtered error for weight updates and guarantees uniform ultimate boundedness of the estimation error, mitigating local overfitting inherent to instantaneous error-based schemes. To evaluate whether the network has learned a consistent, time-invariant nonlinear mapping, a Frozen-Weight Reproducibility Test is introduced, in which past data are replayed using frozen neural network weights. Simulations under step-steer and slalom maneuvers show that the proposed identifier achieves real-time tire force estimation accuracy comparable to a conventional instantaneous error-based scheme, while significantly improving frozen-weight reproducibility and overall model consistency.**

***Index Terms*—Online System Identification, Neural Networks, Nonlinear Dynamics, Vehicle Dynamics, Tire Force Estimation**

I. INTRODUCTION

Accurate estimation of lateral tire forces is essential for advanced vehicle control systems such as autonomous path tracking and stability control [1]–[3]. Because direct measurement of the tire-road interaction is impractical in production vehicles, estimation must be performed online using vehicle dynamics models. However, linear tire models are valid only in the normal handling region and cannot capture saturation effects, while key physical properties vary significantly with load, temperature, and road friction. As a result, real-time estimators that rely on fixed nominal parameters often exhibit large errors in practical driving scenarios.

Existing real-time estimation approaches differ in the quantity they attempt to estimate online:

1) *Disturbance Estimation (Signal Estimation):* Methods such as Extended Kalman Filter and Extended State Observer [2], [3] treat unmodeled tire dynamics as a lumped disturbance or unknown input. These schemes provide robust instantaneous force estimates for state feedback, but they estimate only the *signal* rather than the underlying *force model*. As a consequence, the constitutive relationship between slip, load, and lateral force cannot be reconstructed, limiting their effectiveness for predictive or force-aware control.
2) *Parameter Estimation (Physical model):* These approaches [4] assume a predefined analytic structure such as the Pacejka Magic Formula or Dug-off model and update a small set of parameters (e.g., cornering stiffness or friction coefficients) in real time. While physically interpretable, the fixed structural form restricts accuracy when actual tire behavior deviates from the assumed model due to complex road conditions or extreme maneuvers.
3) *Function Identification (Structure + Parameter Learning):* Data-driven methods [5]–[7], aim to learn the nonlinear mapping $f(\mathbf{x}, \mathbf{u})$ directly from data. This allows full reconstruction of the nonlinear tire behavior. However, conventional online learning relies on instantaneous error minimization, making weight adaptation highly sensitive to noise and transient dynamics, which often leads to parameter drift and unstable updates.

To address the stability issues inherent in instantaneous-error online learning, an integral error-based adaptive neural identifier was recently introduced [8]. By deriving the adaptation law from an exponentially weighted integral cost functional, this method filters high-frequency fluctuations and ensures stable convergence. This work extends that framework to lateral vehicle dynamics for real-time identification of nonlinear lateral tire forces. The proposed method suppresses overfitting to instantaneous residuals and consistently reconstructs the nonlinear tire behavior without requiring ground-truth force measurements.ground-truth force measurements.

II. PROBLEM FORMULATION FOR TIRE FORCE IDENTIFICATION

A. Nominal Linear Bicycle Dynamics

The lateral and yaw dynamics of a single-track vehicle are

$$m(\dot{v}_y + v_x r) = F_{y\mathrm{f}} + F_{y\mathrm{r}}, \tag{1}$$

$$I_z \dot{r} = l_\mathrm{f} F_{y\mathrm{f}} - l_\mathrm{r} F_{y\mathrm{r}}. \tag{2}$$

Under the small-slip assumption, the front and rear lateral tire forces are approximated linearly as

$$F_{yi} = C_{\alpha i}\alpha_i, \quad (i \in \{\mathrm{f}, \mathrm{r}\}), \tag{3}$$

This work was supported in part by the National Research Foundation of Korea (NRF) grant funded by the Korea government (MSIT) (RS-2025-00554087).

where the slip angles are $\alpha_\mathrm{f} \approx \delta_\mathrm{f} - (v_y + l_\mathrm{f} r)/v_x$ and $\alpha_\mathrm{r} \approx \delta_\mathrm{r} - (v_y - l_\mathrm{r} r)/v_x$. Substituting the linearized tire forces from (3) yields the standard 2-DOF linear bicycle model:

$$\dot{\mathbf{x}} = \mathbf{A}\mathbf{x} + \mathbf{B}\mathbf{u}, \qquad \mathbf{x} = \begin{bmatrix} v_y \\ r \end{bmatrix}, \quad \mathbf{u} = \begin{bmatrix} \delta_\mathrm{f} \\ \delta_\mathrm{r} \end{bmatrix}, \tag{4}$$

with the nominal system matrices

$$\mathbf{A} = \begin{bmatrix} -\dfrac{C_{\alpha\mathrm{f}} + C_{\alpha\mathrm{r}}}{m v_x} & -v_x - \dfrac{C_{\alpha\mathrm{f}} l_\mathrm{f} - C_{\alpha\mathrm{r}} l_\mathrm{r}}{m v_x} \\ -\dfrac{C_{\alpha\mathrm{f}} l_\mathrm{f} - C_{\alpha\mathrm{r}} l_\mathrm{r}}{I_z v_x} & -\dfrac{C_{\alpha\mathrm{f}} l_\mathrm{f}^2 + C_{\alpha\mathrm{r}} l_\mathrm{r}^2}{I_z v_x} \end{bmatrix},$$

$$\mathbf{B} = \begin{bmatrix} \dfrac{C_{\alpha\mathrm{f}}}{m} & \dfrac{C_{\alpha\mathrm{r}}}{m} \\ \dfrac{C_{\alpha\mathrm{f}} l_\mathrm{f}}{I_z} & -\dfrac{C_{\alpha\mathrm{r}} l_\mathrm{r}}{I_z} \end{bmatrix}.$$

While this linear model captures the basic handling dynamics, it fails to represent the nonlinear tire behaviors arising from load transfer, friction variations, and saturation limits in real-world driving. However, in real driving environments, the lateral tire forces exhibit significant nonlinearities due to:

- load transfer and varying vertical loads,
- variations in road friction coefficient (μ),
- tire temperature and pressure changes,
- force saturation at large slip angles.

Thus, the nominal linear model (4) cannot accurately capture the full range of tire behavior.

B. Nonlinear Tire Effects and Bicycle Model

To represent deviations from the linearized forces due to saturation or friction changes, unknown nonlinear functions f_i ($i \in \{f, r\}$) is introduced as:

$$F_{yi} = C_{\alpha i}\alpha_i + f_i(\delta_i, v_x, v_y, r). \tag{5}$$

Defining the nonlinear term vector as $\boldsymbol{f}(\mathbf{x}, \mathbf{u}) = [f_\mathrm{f}, f_\mathrm{r}]^\top$, the nonlinear bicycle model is expressed as:

$$\dot{\mathbf{x}} = \mathbf{A}\mathbf{x} + \mathbf{B}\mathbf{u} + \mathbf{K}\boldsymbol{f}(\mathbf{x}, \mathbf{u}), \tag{6}$$

where the input matrix is $\mathbf{K} = [\frac{1}{m}, \frac{1}{m}; \frac{l_\mathrm{f}}{I_z}, -\frac{l_\mathrm{r}}{I_z}]^\top$.

C. Problem Statement for Neural Identification

Direct identification of $\boldsymbol{f}$ in (6) is challenging because the matrix $\mathbf{K}$ couples the unknown tire forces to both state derivatives (v_y and r). To decouple these terms, we introduce a linear state transformation $\xi = \mathbf{K}^{-1}\mathbf{x}$. Since $\det(\mathbf{K}) \neq 0$, this transformation is valid. The dynamics in the transformed domain are obtained as:

$$\dot{\xi} = \mathbf{A}_\xi \xi + \mathbf{B}_\xi \mathbf{u} + \boldsymbol{f}(\mathbf{x}, \mathbf{u}), \tag{7}$$

where $\mathbf{A}_\xi := \mathbf{K}^{-1}\mathbf{A}\mathbf{K}$ and $\mathbf{B}_\xi := \mathbf{K}^{-1}\mathbf{B}$. This canonical form isolates the nonlinearity $\boldsymbol{f}$ as a matched uncertainty, enabling component-wise approximation without inverting $\mathbf{K}$ inside the adaptive loop.

III. Integral Error-Based Neural Identifier

A. Identifier Design

To guarantee stable online identification where the true values of the nonlinear dynamics are unmeasurable, a Luenberger-like observer framework is employed. The core strategy utilizes the state estimation error as the driving force for the weight adaptation. By enforcing the error dynamics to be governed by a user-defined Hurwitz matrix $\mathbf{A}_d$, any persistent estimation error is driven solely by the inaccuracy of the neural network weights.

Based on the transformed dynamics (7), the proposed identifier structure is given by:

$$\dot{\hat{\xi}} = \underbrace{\mathbf{A}_d \hat{\xi}}_{\text{stable error dynamics}} + \underbrace{(\mathbf{A}_\xi \xi + \mathbf{B}_\xi \mathbf{u} - \mathbf{A}_d \xi)}_{\text{known dynamics feedforward}} + \hat{\boldsymbol{f}}(\hat{\mathbf{x}}, \mathbf{u}). \tag{8}$$

This structure consists of three key components:

a) Prescribed Error Dynamics: : The term $\mathbf{A}_d \hat{\xi}$ imposes strictly stable linear dynamics on the estimator. The Hurwitz matrix $\mathbf{A}_d$ is designed to govern the convergence rate of the estimation error, independent of the system's physical parameters.

b) Known Dynamics Feedforward: : The bracketed term utilizes measured states to compensate for the modeled system dynamics, effectively isolating the unknown residual nonlinearity for the neural network.

c) Neural Approximation: : The term $\hat{\boldsymbol{f}}$ represents the neural network designed to approximate the residual nonlinearity. It is defined as $\hat{\boldsymbol{f}} = \hat{\mathbf{W}}\sigma(\hat{\mathbf{V}}\hat{\bar{\mathbf{x}}})$, where $\hat{\mathbf{W}}$ and $\hat{\mathbf{V}}$ are the estimated weight matrices, and $\sigma(\cdot)$ is the element-wise $\tanh$ activation function. The input vector $\hat{\bar{\mathbf{x}}} = [\hat{\mathbf{x}}^\top, \mathbf{u}^\top]^\top$ utilizes estimated physical states.

B. Adaptive Law

Conventional online neural identifiers minimize the instantaneous squared error $\|\tilde{\xi}(t)\|^2$, which makes the weight update highly sensitive to noise and local variations [5]. Instead, the following integral cost functional is considered in the transformed domain:

$$J(t) = \frac{1}{2}\int_0^t e^{-\lambda(t-\tau)}\tilde{\xi}^\top(\tau)\tilde{\xi}(\tau)\, d\tau, \tag{9}$$

where $\lambda > 0$ is a forgetting factor. This formulation emphasizes recent errors while still incorporating past information.

Define the filtered error signal in the transformed domain as

$$\mathbf{z}(t) = \int_0^t e^{-\lambda(t-\tau)}\tilde{\xi}(\tau)\, d\tau, \tag{10}$$

which satisfies the differential equation $\dot{\mathbf{z}} = -\lambda\mathbf{z} + \tilde{\xi}$.

Using $\mathbf{z}$, the gradient of the integral cost with respect to the estimation error is

$$\frac{\partial J}{\partial \tilde{\xi}} = \mathbf{z}^\top.$$

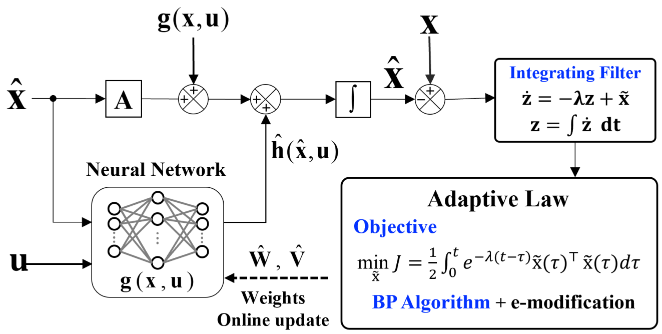

Fig. 1: Integral error based NN-Identifier scheme.

By employing the backpropagation-based gradient descent method alongside the static approximation technique detailed in [5], [8], the adaptive update laws are derived as:

$$\dot{\hat{\mathbf{W}}} = -\eta_1 \left(\mathbf{z}^\top \mathbf{A}_d^{-1}\right)^\top \sigma(\hat{\mathbf{V}}\hat{\bar{\mathbf{x}}})^\top - \rho_1 \|\tilde{\xi}\| \hat{\mathbf{W}}, \tag{11}$$

$$\dot{\hat{\mathbf{V}}} = -\eta_2 \left(\mathbf{z}^\top \mathbf{A}_d^{-1} \hat{\mathbf{W}} (\mathbf{I} - \boldsymbol{\Lambda})\right)^\top \hat{\bar{\mathbf{x}}}^\top - \rho_2 \|\tilde{\xi}\| \hat{\mathbf{V}}, \tag{12}$$

where $\eta_1, \eta_2 > 0$ are learning rates and $\rho_1, \rho_2 > 0$ are leakage gains ensuring robustness. The diagonal matrix

$$\boldsymbol{\Lambda} = \mathrm{diag}\left\{\sigma_i^2(\hat{\mathbf{V}}_i \hat{\bar{\mathbf{x}}})\right\} \tag{13}$$

arises from the derivative of the activation function. Note that while the error $\tilde{\xi}$ is in the transformed domain, the input vector $\hat{\bar{\mathbf{x}}}$ typically consists of the estimated physical states $\hat{\mathbf{x}}$.

C. Stability Analysis

Using a Lyapunov function that incorporates the transformed state estimation error $\tilde{\xi}$ together with the weight estimation errors, it can be shown (with the detailed derivation provided in [8], [5]) that the closed-loop error system under the adaptive laws (11)–(12) guarantees uniform ultimate boundedness of $\tilde{\xi}$. More specifically, the estimation error $\tilde{\xi}$ converges to a compact set whose radius is upper bounded by

$$\|\tilde{\xi}\| \le b := \frac{2\left(\|P\|\bar{w} + k_b^2\right)}{\lambda_{\min}(Q)}, \tag{14}$$

where $Q = -(A_d^\top P + P A_d)$ is positive definite, $\bar{w}$ is an upper bound on the NN approximation error, and k_b is a constant determined by the learning rates (η_1, η_2) and the leakage gains (ρ_1, ρ_2).

Since both P and the design matrix A_d are user-chosen parameters, the ultimate bound radius b can be tuned directly.

IV. Validation

This section evaluates the performance of the proposed integral error-based adaptive neural identifier through high-fidelity vehicle simulations. The comparative study benchmarks the proposed *integral error-based* scheme against the conventional *instantaneous error-based* adaptive NN identifier.

A. Evaluation Methodology

To distinguish true structural identification from transient local overfitting, we introduce a novel validation procedure termed the **Frozen-Weight Reproducibility Test**.

The procedure consists of three stages:

1) *Online Adaptation Phase:* The identifier trains the neural network online continuously up to a specific time instance T_{freeze}.
2) *Weight Freezing:* At $t = T_{\text{freeze}}$, the adaptation law is deactivated, and the weights are fixed at their instantaneous values $\hat{\mathbf{W}}(T_{\text{freeze}}), \hat{\mathbf{V}}(T_{\text{freeze}})$.
3) *Feedforward Re-evaluation:* The historical data is re-evaluated using these frozen weights. The network output $\hat{\mathbf{f}}(\mathbf{x}, \mathbf{u}; \hat{\mathbf{W}}_{\text{frozen}}, \hat{\mathbf{V}}_{\text{frozen}})$ is compared against the original outputs generated during the active adaptation phase.

The underlying intuition is that if the network has meaningfully learned the dynamics within its operating region, the output generated by the frozen weights must identically reproduce the historical estimation results for $t < T_{\text{freeze}}$. Any discrepancy implies that the weights were merely overfitting to instantaneous residuals rather than capturing the consistent physical structure.

B. Simulation Setup and Scenarios

The validation is conducted within the IPG CarMaker environment, an industry-standard high-fidelity vehicle dynamics simulation software. The target vehicle is modeled as a representative commercial mid-size sedan. The vehicle configuration incorporates full multi-body dynamics, including suspension kinematics, compliance, and load transfer effects. The ground-truth tire forces are generated using the Pacejka Magic Formula 5.2 model.

The proposed neural identifier is implemented in MATLAB/Simulink and co-simulated with CarMaker at a sampling interval of $T_s = 0.01\,\mathrm{s}$. The network architecture consists of a single hidden layer with hyperbolic tangent ($\tanh$) activation functions.

To evaluate the identifiers under varying dynamic conditions, two maneuvers are employed:

- *Step-Steer maneuver:* This scenario induces a rapid buildup of tire forces followed by a quasi-steady-state condition. It is designed to evaluate the adaptation rate during the transient phase and the estimation stability in the steady-state phase.
- *Slalom maneuver:* This scenario generates continuous time-varying lateral dynamics. It is designed to assess the structural consistency of the learned model and its ability to retain historical information without parameter drift.

C. Performance Analysis: Step-Steer Maneuver

Figs. 2 and 3 present the comparative results for the Step-Steer maneuver. The top subplots show the online estimation performance, while the bottom subplots show the validation results with frozen weights.

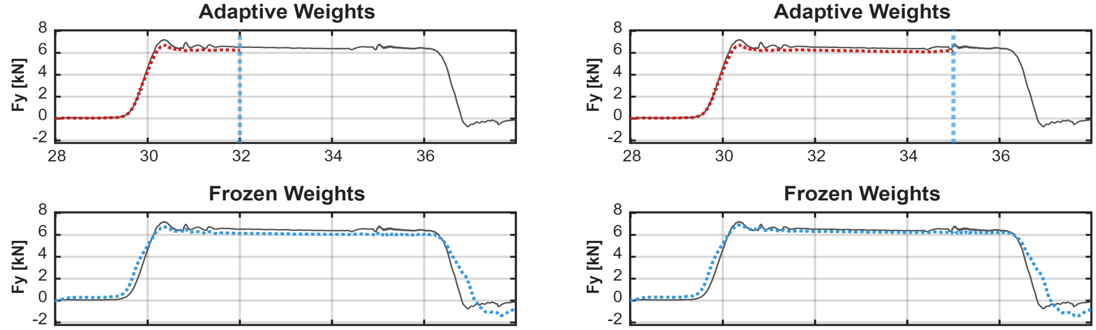

(a) Weight adaptation is active until $t = 32s$.

(b) Weight adaptation is active until $t = 35s$.

Fig. 2: Results of the **Instantaneous** error-based NN-identifier (Step-Steer). In each subplot, the top graph shows online estimation($\cdots$) and the bottom graph shows validation($\cdots$) with frozen weights.

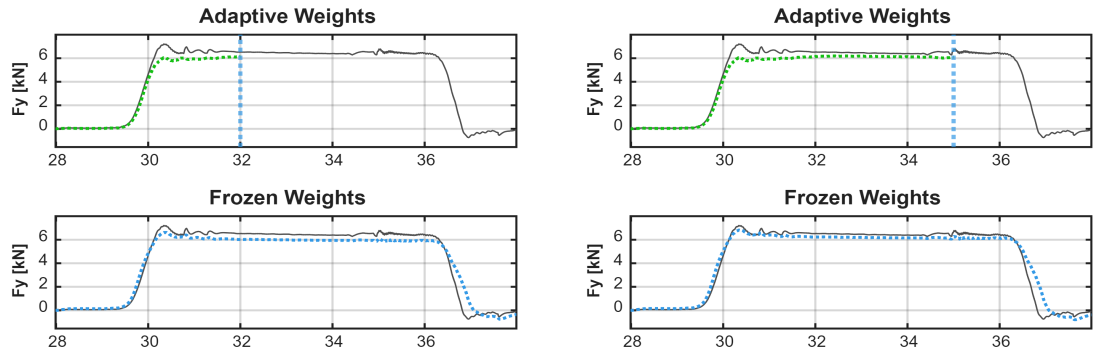

(a) Weight adaptation is active until $t = 32s$.

(b) Weight adaptation is active until $t = 35s$.

Fig. 3: Results of the **Integral** error-based NN-identifier (Step-Steer). In each subplot, the top graph shows online estimation($\cdots$) and the bottom graph shows validation($\cdots$) with frozen weights.

a) Instantaneous Error-Based Method (Fig. 2): While the online estimation (top) appears to track the ground truth reasonably well, the frozen-weight validation (bottom) shows that the transient behavior learned earlier is partially forgotten as the system moves into the near–steady-state region. With weights frozen at $t = 32\,\mathrm{s}$, the steady-state level is reproduced, but the step-induced transient slope around $t = 29$–$30\,\mathrm{s}$ is not. A similar loss of transient behavior is observed when the weights are frozen at $t = 35\,\mathrm{s}$, indicating that the instantaneous-error scheme does not preserve the transient mapping once the operating conditions change.

b) Integral Error-Based Method (Fig. 3): In contrast, the proposed method demonstrates superior consistency. Regardless of whether the weights are frozen at $t = 32s$ or $t = 35s$, the frozen model reproduces the historical estimation trajectory with high fidelity. This confirms that the integral action effectively filters out high-frequency fluctuations, allowing the weights to converge to a stable solution.

However, the mismatch observed after $t = 36\,\mathrm{s}$ indicates that both methods have limited predictive capability outside the time interval in which the weights were adapted, although the proposed method still exhibits high reproducibility within the region where training actually occurred.

D. Performance Analysis: Slalom Maneuver

The limitation of the instantaneous approach becomes most apparent in the Slalom maneuver, where the system states change rapidly.

a) Instantaneous Error-Based Method (Fig. 4): Fig. 4 illustrates the failure of the instantaneous identifier. During the online phase (top), the estimation seems accurate. However, in Fig. 4a (frozen at $t = 32s$), the neural network completely fails to reproduce the forces observed in the earlier phase ($t < 30s$) and only matches the dynamics near $t = 32s$. Fig. 4b (frozen at $t = 40s$) shows a similar pattern. This indicates that the weight adaptation is strongly influenced by the instantaneous error, leading to loss of previously acquired mappings. Consequently, the "learned model" at $t = 32s$ and $t = 40s$ are only valid for that specific instant and have no predictive power for the true dynamics.

b) Integral Error-Based Method (Fig. 5): Conversely, the proposed integral error-based identifier exhibits noticeable reproducibility. The frozen response (dashed blue line) overlays

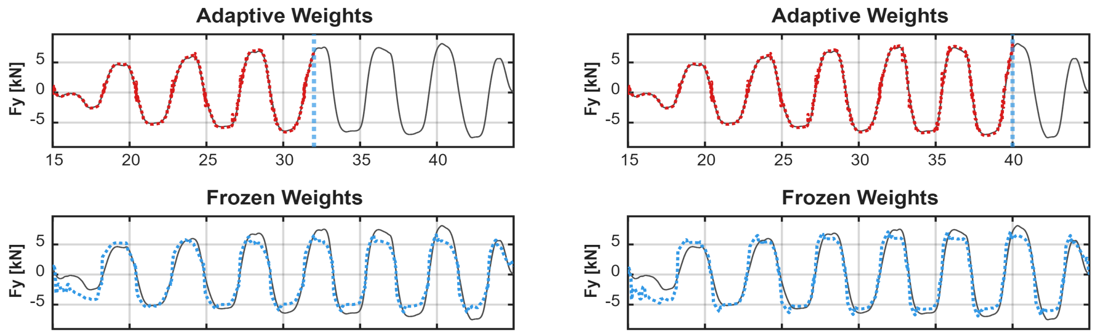

(a) Weight adaptation active until $t = 32s$.

(b) Weight adaptation active until $t = 40s$.

Fig. 4: Results of the **Instantaneous** error-based NN-identifier (Slalom). In each subplot, the top graph shows online estimation($\cdots$) and the bottom graph shows validation($\cdots$) with frozen weights.

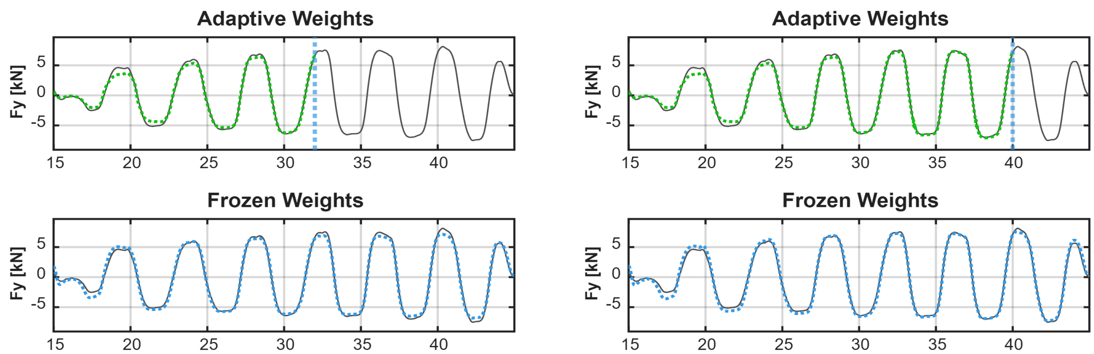

(a) Weight adaptation active until $t = 32s$.

(b) Weight adaptation active until $t = 40s$.

Fig. 5: Results of the **Integral** error-based NN-identifier (Slalom). In each subplot, the top graph shows online estimation($\cdots$) and the bottom graph shows validation($\cdots$) with frozen weights.

the online estimation (solid line) across the entire history, independent of the freezing timestamp ($t = 32s$ or $t = 40s$). This result indicates that the integral error term forces the weight update to respect the accumulation of past errors. By doing so, it prevents the weights from chasing transient noise and ensures that the neural network learns the time-invariant nonlinear structure of the tire dynamics.

E. Summary of Validation Results

The comparative analysis, summarized in Tables I and II, clearly demonstrates the good model consistency of the proposed Integral Error-Based method. While the online tracking performance remains largely comparable across both maneuvers, a divergence is observed in model consistency. In the highly dynamic Slalom maneuver (II), the Instantaneous scheme exhibits structural instability in the Frozen-Weight Reproducibility Test, failing to consolidate the learned model. Even in the simpler Step Steer case (I), the Integral method demonstrates superior weight consistency, validating its ability to successfully maintain the model structure. This collective evidence confirms that the integral cost functional successfully enforces the learning of a reliable, time-invariant functional mapping essential for robust predictive control.

TABLE I: Validation of Learned Tire Models under Step Steer Maneuver

Step Steer Maneuver		
Metric (Condition)	**Instantaneous** (Conventional)	**Integral** (Proposed)
Online Estimation	**0.2690 kN**	0.4077 kN
Frozen Weights ($32s$)	0.6506 kN	**0.5562 kN**
Frozen Weights ($35s$)	0.6488 kN	**0.5015 kN**

[a] Values represent the Root Mean Square Error (RMSE)

V. Conclusion

This paper presented an integral error-based adaptive neural identifier for real-time estimation of nonlinear lateral tire forces. Conventional neural identifiers rely on instantaneous error minimization, which makes their weight updates highly sensitive to noise and often leads to local overfitting. The Frozen-Weight Reproducibility Test showed that such overfitting causes the learned model to lose previously acquired

TABLE II: Validation of Learned Tire Models under Slalom Maneuver

Slalom Maneuver		
Metric **(Condition)**	**Instantaneous** (Conventional)	**Integral** (Proposed)
Online Estimation	0.3388 kN	**0.3386 kN**
Frozen Weights ($32s$)	1.4529 kN	**0.4247 kN**
Frozen Weights ($40s$)	1.5332 kN	**0.4300 kN**

[a]Values represent the Root Mean Square Error (RMSE)

information once the operating conditions change, indicating a lack of structural consistency. In contrast, the proposed method uses an integral cost functional for adaptation, which prevents this forgetting effect and enables the network to retain the relationships learned from past operating conditions rather than reacting only to transient residuals. Simulation results demonstrated that the proposed framework achieves accurate real-time estimation while consistently reproducing the nonlinear tire dynamics across different operating regimes. This property makes it suitable for safety-critical applications, particularly predictive control strategies that require stable and reliable force models over time.

References

[1] W. Cho, J. Yoon, S. Yim, B. Koo, and K. Yi, "Estimation of tire forces for application to vehicle stability control," *IEEE Transactions on Vehicular Technology*, vol. 59, no. 2, pp. 638–649, 2010.

[2] L. Ray, "Nonlinear state and tire force estimation for advanced vehicle control," *IEEE Transactions on Control Systems Technology*, vol. 3, no. 1, pp. 117–124, 1995.

[3] L.-H. Zhao, Z.-Y. Liu, and H. Chen, "Design of a nonlinear observer for vehicle velocity estimation and experiments," *IEEE Transactions on Control Systems Technology*, vol. 19, no. 3, pp. 664–672, 2011.

[4] G. Torres-Charry and J.-B. Gómez-Mendoza, "Static friction in a cable-driven transmission—modeling and identification of load effects," *Lubricants*, vol. 10, no. 5, 2022. [Online]. Available: https://www.mdpi.com/2075-4442/10/5/100

[5] F. Abdollahi, H. A. Talebi, and R. V. Patel, "Stable identification of nonlinear systems using neural networks: Theory and experiments," *IEEE/ASME Transactions on Mechatronics*, vol. 11, no. 4, pp. 488–495, Aug 2006.

[6] J. Jia, W. Zhang, K. Guo, J. Wang, X. Yu, Y. Shi, and L. Guo, "Evolver: Online learning and prediction of disturbances for robot control," *IEEE Transactions on Robotics*, vol. 40, pp. 382–402, 2024.

[7] H. Talebi, R. Patel, and H. Asmer, "Neural network based dynamic modeling of flexible-link manipulators with application to the ssrms," *Journal of Robotic Systems*, vol. 17, pp. 385 – 401, 07 2000.

[8] D. Hong and K. Choi, "Integral error-based adaptive neural identifier for a class of uncertain nonlinear systems," *TechRxiv*, Jul 2025, preprint.